A High Sensitive Nanomaterial Coated Side Polished Fiber Sensor for Detection of Cardiac Troponin I Antibody

M.Valliammai, J.Mohanraj, Balasubramanian Esakki, Lung-Jieh Yang, Chua-Chin Wang and A.Bakiya

***Abstract*— The advent of evanescent field based fiber optic biosensor and advancements in nanotechnology has create an excellent opportunity in label-free detection of biomarkers which plays vital role in the early, rapid and accurate diagnosis of acute diseases. In this work, we demonstrate a high sensitive Molybdenum Tungsten Disulfide ($MoWS_2$) coated side polished fiber (SPF) biosensor for accurate and early diagnosis of cardio vascular disease (CVD). The Cardiac Troponins I (cTnI) is identified as a biomarker of interest for early and rapid diagnonis of CVD. The proposed SPF biosensor exhibits surface plasmonic resonance (SPR) detection due to the evanescent field interaction between $MoWS_2$ nano coated side polished region and anti-CTnI. The proposed SPF biosensor possess the high sensitivity of 82% to detect the cTnI antibody with a limit of detection (LOD) about 17.5 pg/mL. The peak SPR shift have been calculated as 61 nm for analyte concentrations of 500 pg/mL Moreover, the proposed SPF biosensor possess the high degree of selectivity and environmental stability to CTnI among three analytes such as CTnI, Estrogen and Glucose. The hydrophobic interactions of $MoWS_2$ and cTnI antibody leads to chemical free biofunctionalization of antibody in the sensing region. Hence, the simulation results shows the surface interaction strength calculated as 1.29 KJ mol^{-1}/nm^2 in order to evaluate the hydrophobic interactions. Thus, the proposed optical biosensor is a promising candidate for "point-of-care" testing of CVD disorders and preclinical assessments.**

***Index Terms*— Side polished fiber, Molybdenum Tungsten Disulfide nanomaterial, Surface plasmonic resonance and Cardiac Troponin I**

I. Introduction

THE world health organization (WHO) states that CVD is a noncommunicable diseases and reponsible for demise of people around 17.9 million per year [1], [2]. CVD leads to a hypertension, high risk of stroke, coronary heart diseases and chronic vascular disorders. An accurate diagnosis of CVD is critical because that occur suddenly and progress rapidly. Hence, accurate, rapid and timely diagnosis for CVD is highly essential for progression of clinical treatment. Recently, the various optical detection method such as fluorescence resonance energy transfer, chemiluminescence and surface-enhanced Raman scattering (SERS) have been used in the current trend for detection of CVD [3]. Firstly, Benford et al. have been demonstrated the SERS based assay analyzation for three cardiac biomarkers (BNP, cTnI, and CRP) for diagnosing acute coronary syndrome [4]. Further, cTnI have been identified by SER spectroscopy in the mapping test region [5]. Nevertheless, SERS possesses the weak Raman spectrum for lower concentrations of biomarkers [6]. The advent of optical fiber biosensors becomes as a feasible candidate for improved LOD, portability, light weight, biocompatibility and immune to electromagnetic interference [7], [8]. Lately, T. Liu et al. demonstated the phase shifted micro fiber grating based CVD biomarker detection with a LOD of 0.03 ng/mL [9]. To date, LOD of particular biomarkers relative to the optical fiber biosensors have improved by the phenomenon SPR. This effect have achieved by nano-material coated optical fibers in sensing region which exhibits the high reproducibility and degree of accuracy in the LOD measurement [10]. The SPR can occur when real part value of the nano-material permittivity has to be negative. Further, SPR based sensors can excite transverse electric or magnetic modes and can enable a label-free method to analyze the real time bioanalytes interactions. In recent past, various optical fiber biosensor structures such as tapered [11], U-shape [12] and side polished [13] have been used to obtain the effect of SPR for the improved LOD and high sensitivity of biomarker [3]. Among these, SPF has enhanced evanescent field due to polished region of clad. Hence, we have a choice of SPF not only for high evanescent field interaction but also which requires a very small quantity of sample in the sensing region with improved LOD. Consequently, we intend to exploit use of SPR effect on SPF based biosensor.

Over the past decade, transition metal dichalcogenides (TMDs) nano particles take place role to exhibit SPR effect with good specificity and environmental stability in optical biosensor [14], [15]. Among the various Transition metal dichalcogenides (TMDs), the potential of MoS_2 and WS_2 nanosheets are widely reported for biosensing applications. In the recent past, our report [16] has shown that $MoWS_2$ nano composite coated all-optical multi gas sensor for environmental applications. Subsequently, we have a intend to utilize the advantages of $MoWS_2$ in optical biosensor in order to improve its sensitivity with SPR effect for CVD accurate diagonosis. Further, we have a choice of $MoWS_2$ to exploit the advantages of MoS_2 and WS_2 such as large surface area, biocompatibility, superior hydrophobic interactions, excellent affinity with biomarkers and catalytic activity [10], [17]–[19]. Nevertheless, detecting cardiac biomarkers poses a significant challenge due to their extremely low concentrations. In particular, CTnI and Cardiac Troponins T (cTnT) are well-recognized biomarkers for assessing the acute heart failure [20]. Recently, we have demonstrated the high sensitive $MoWS_2$ nanocoated SPF biosensor for detection of CTnT [21]. Here, we have a intend to work on cTnI which more precisely associated with acute myocardial infarction and heart attacks and failure. The concentration of cTnI in human blood typically $\geq$ 0.01 ng/mL, depending on the chronicity of CVD disorders [9], [22], [23]. In the recent years, immunosensor have reported to measure the cardiac Troponin concentration [24]. Nevertheless, the low LOD for Troponins using optical detection such as immunofluorescence, chemiluminescence is complex process [24]. Hence, We belive that the properties of $MoWS_2$ nanomaterial and SPF act as a promising candidate for accurate detection of CTnI antibodies with ultra-low

This research was funded by the Department of Science and Technology (DST) - Global Innovation and Technology Alliance (GITA), Government of India under the call for proposal 2021 India-Taiwan S & T cooperation (GITA/DST/TWN/P-99/2022).

M.Valliammai, J. Mohanraj and A. Bakiya are with the department of Electronics and Communication Engineering, Vel Tech Rangarajan Dr. Sagunthala R&D Institute of Science and Technology, Chennai, India (e-mail: classicvalli@gmail.com;mohanvit.86@gmail.com;bakiya88@gmail.com).

Balasubramanian Esakki is with the department of Mechanical Engineering, National Institute of Technical Teachers Training and Research, Chennai, India (e-mail: esak.bala@gmail.com).

Lung – Jieh Yang is with the department of Mechanical Engineering,Tamkang University, New Taipei, Taiwan (e-mail: ljyang@mail.tku.edu.tw).

Chua-Chin Wang is with department of Electrical Engineering,National Sun Yat-Sen University, Kaohsiung, Taiwan (e-mail: ccwang@ee.nsysu.edu.tw).

concentration.

In this work, we have demonstrated a nano coated SPF biosensor for accurate detection of CTnI anti bodies. To the author's knowledge, this work represents the first demonstration on $MoWS_2$ nanocoated SPR based SPF biosensor for cTnI antibody detection. Further, the interfacing of few layer $MoWS_2$ nano composites facilitates the rapid and chemical free antibodies immobilization on sensing region of SPF due to its hydrophopic interaction.Furthermore, the proposed $MoWS_2$ coated biosensor detects the CTnI concentration with a high sensitivity of 82% and its LOD of 17.5 pg/mL. These features of proposed biosensor open the way for POC device development for early and accurate diagnosis of CVD disorders. The article has been organized as follows: Section II. deals with the synthesis characterization of $MoWS_2$. Further, section 7. shows the fabrication of device and experiment analysis of proposed SPF biosensor for the detection of cTnI antibody. In the Section IV, the SPR wavelength shift as well as the LOD for the various concentration of cTnI biomarker and numerical investigation of hydrophopic interaction is analysed. Finally, the research finding concluded with the section.V

II. SYNTHESIS AND CHARACTERIZATION

$MoWS_2$ nanomaterials have been synthesized using hydrothermal exfoliation method [25]. This process involves mixing of 3.85 mmol of sodium molybdenum oxide dehydrate (Na-$2MoO_4.2H_2O$), 15mmol of thiocarbamide (CH_4N_2S), 0.15 mmol of sodium tungstate dehydrate ($Na_2WO_4.2H_2O$), 4.029 mmol of Hydroxylamine hydrochloride (H_3NoHcl) and 15 mmol of oxalic acid ($H_2C_2O_4$). Deionised (DI) solvent is added with the resulting bulk nanomaterial mixture and subjected to stir continuously for one hour. The solution is then filled into 50 ml Teflon lined home made autoclave that placed inside a hot air furnace set to 250°C up to a duration of 28 hours. The remnants from the autoclave are acquired and cleansed using ethanol. Subsequently, DI solvent is used to eliminate any undesired residues. Further, the sample is subjected to a hot air oven at 75°C for a duration of 15 hours. Following this, the sample is finely powdered using an agate jar and the concentration of 20 mg/ml N-methyl 2-pyrrolidone solvent is used to dissolve the residue. The sample is then subjected to the ultrasonification process with the time interval of 2 hours for 3 times. Further, washing and cleaning the impurities are repeated for 5 times. Finally, the sample is dried using vacuum drying for 4 hours at 80°C. Ultimately, the resulting solution is a $Mo_{(1-x)}W_xS_2$ few-layer composite which fabricated with a ratio of x equal to 0.2, which can be seen in pastel green color. The primary challenge of growing the emerging 2D semiconductor $MoWS_2$ lies in controlling the layer thickness and preventing the atomic bonding with the monolayer. Additionally, visualizing the elemental distribution at the atomic level poses a significant challenge. Furthermore, achieving a tunable composition for $MoWS_2$ requires careful consideration of the precursor heating duration, which directly impacts the distribution of Mo and W atoms on the $MoWS_2$ heterostructure's surface.

The fabricated $MoWS_2$ heterostructure represents a recently investigated material to explore its characteristics. Despite exhibiting preferable chemical, photonic and electronic properties, further analysis is required to assess its preparation and compatibility methods. Additionally, addressing the challenges associated with this nanosheet involves structural analysis, including lattice mismatch, gap states as well as electronic characteristics such as mobility and conductivity. Moreover, it is essential to investigate the stability of the synthesized nanosheet in response to environmental elements such as humidity, temperature and moisture. Further, there is need of research for study

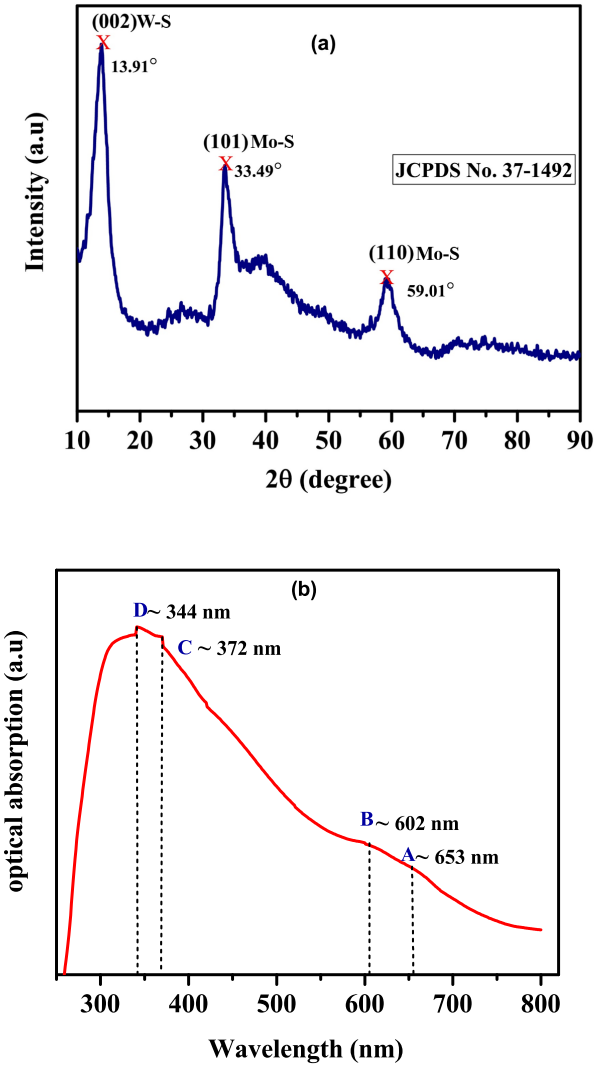

Fig. 1. (a) XRD analysis synthesized $MoWS_2$ sample. (b) UV-Vis absorption analysis of $MoWS_2$ sample.

the various such as biocompatibility and cytotoxicity of $MoWS_2$. Nonetheless, the investigation of biocompatibility of MoS_2 and WS_2 possess that these are suitable candidates for bio sensing system because of its low cytotoxicity and genotoxicity [26]. Hence, we intend to newly explore the benefit of hybrid structure of $MoWS_2$ in bio-sensing applications.

A. Characterization of $MoWS_2$ nanosheet

The validation of the $MoWS_2$ nanosheet presence was carried out through X-ray diffraction (XRD) study using a Bruker D8 Advance instrument by fixing an optimum wavelength as 1.5406 Å. Additionally, in order to verify the identity of the $MoWS_2$ synthesized sample, UV-Vis spectroscopy was conducted with a spectrophotometer (JASCO-V-670) with a covering wavelengths from 300 nm to 1700 nm. The synthesized $MoWS_2$ structure have analysed by field emission scanning electron microscopy (FESEM) with a Hitachi SU8220. Further, the HRTEM using Tecnai G2 20 twin was utilized to assess the nanosheet structure, while EDX was performed to infer the composition of the $MoWS_2$ sample.

The structural characteristics of the synthesized $MoWS_2$ sample were initially analyzed using XRD. Specifically, the crystalline structure of the material was validate by the XRD spectra presented in Fig.1 (a). The trend of spectra exhibits the distinct peaks at 13.91°, 33.49°, and 59.01°, corresponding to the [0 0 1], [1 0 1], and [1 1 0] planes, respectively. Remarkably, these peaks closely resembled those matched with hexagonal (JCPDS Card No. 37-1492) MoS_2 [27], indicating structural similarity between the synthesized material and MoS_2. Additionally, the spectra revealed significant diffraction peaks. This suggests a high level of crystalline structure in the $MoWS_2$ sample. Moreover, the observed peak of the $MoWS_2$ sample is [0 0 2] plane that slightly shifted compared to the standard peaks of MoS_2 and WS_2 that are located at 14.38° and 14.32°, respectively. The slight shift in the observed peak indicates the existing of strain within the inter-layer gap of the fabricated $MoWS_2$, which resulting from the insertion of W atoms inserted between the Mo and S bonds. This observation confirms the presence of few-layered MoWS2 nanosheets in the synthesized solution [16], [28].

Subsequently, the UV-Vis analysis was conducted, and the findings are depicted in Fig. 1 (b). The UV-Vis resuts reveals four distinct peaks located approximately at 653 (A), 602 (B), 372 (C), and 344 nm (D). One can observe the a partial resemblance to the established MoS_2 peaks at approximately 665 (A), 605 (B), 440 (C), and 395 nm (D) with aforementioned $MoWS_2$ peaks [29]. This similarity arises partially owing to the presence of W atoms situated center of the Mo-S bonds. Upon comparison between the peaks of the $MoWS_2$ sample and the standard MoS_2 peaks, it is evident that the peaks of A as well as B coincide, while Peaks C and D demonstrate a blue shift.The observed blue shift can be attributed to alterations in the concentration of the solution resulting from the incorporation of W atoms into the Mo-S bonds. Additionally, this analysis serves to verify that the fabricated sample is indeed a $MoWS_2$ nanosheets.

Furthermore, TEM analysis was conducted to examine the morphology of the prepared $MoWS_2$ nanolayers, as illustrated in Fig.2 (a). The figure shows that the nanolayers have an thickness as approximately 3 nm, suggesting the formation of tightly stacked layers, with each layer measuring around 0.615 nm in thickness. Additionally, the image exhibits sharp edges, confirming the hexagonal shape and crystalline nature of the nanosheets. Subsequently, EDX analysis was performed, confirming the presence of Mo, W, and S atoms in the fabricated $MoWS_2$ nanosheets, as depicted in Fig.2(b). Moreover, characterization using TEM and EDX reveals the tightly enclosed thin film sheets. Additionally, the inset of the Fig.2(b) shows the elemental composition of sample prepared, further confirming the presence of Mo, W, and S atoms.

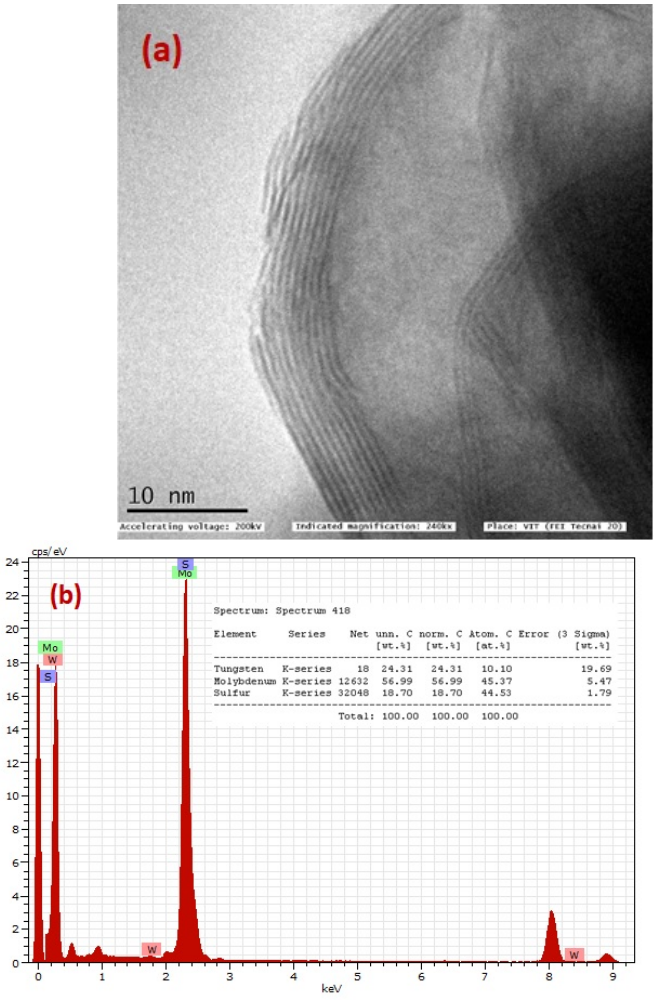

Fig. 2. (a)TEM schematic view of the $MoWS_2$ nano layers (b) synthesized $MoWS_2$ sample elemental composition.

III. Fabrication of Device and its Sensing Behaviour

This section is mainly deals with the fabrication of $MoWS_2$ nano coated biosensor and its sensing characteristics. The device fabrication and sensing measurement comprises the three major processes are explained as follows:

A. Functionalization of $MoWS_2$ Nanosheets on SPF

The proposed biosensor is fabricated by a SPF which has procured from Phoenix photonics. The SPF is a single mode fiber (HI 1060) has core and clad diameters as 8.2 μm and 125 μm, respectively. The clad upper portion has polished approximately $\approx$ 26 mm in length. On the same hand, the above core is polished for a surface length about $\approx$ 17 mm and a depth of $\approx$ 58 μm. Thus, the cladding thickness from the outer surface of the core is approximately 0.4 μm. Consequently, the evanescent field in the SPF is significantly enhanced due to its reduced thickness of clad, which is crucial for the development of high sensitivity biosensors.

The sensitive region of the fiber, which was side-polished, underwent cleaning using a piranha solution (H_2SO_4 / H_2O_2) for 3 minutes at 70°C. The deposition of the $MoWS_2$ solution was carried out using an automated controlled flow system employing a syringe pump (Mindray uSP) in the sensing region of the SPF. Throughout this procedure, the $MoWS_2$ nanosheets were incubated with a total volume of 1mL solution. Optimization of the nanosheets functionalization involved a flow rate of 0.2ml/5mins for 5 cycles. Each cycle comprised the injection of $MoWS_2$ dispersed solution onto the SPF followed by a 5-minute drying period. Subsequently, the sensing region underwent annealing for 60 minutes at 60°C after each cycle to ensure proper coating of $MoWS_2$ nanosheet. Furthermore, the scanning electron microscopy (SEM) image confirms the layer coating of $MoWS_2$ in the sensing region of SPF, as depicted in Fig.3(a) and (b).

B. Protocol for Bioassay functionalization of cTnI antibody on $MoWS_2$ nano coated SPF

The Fig.4 shows the step-by-step process of bioassay functionalization on the $MoWS_2$ nanolayer coated SPF as follows: Initially, $MoWS_2$ nano coated SPF is safely placed inside the microfluidic chamber. The resonance wavelength is observed before functionalization of the CTnI antibodies with 2ml of phosphate-buffered solution

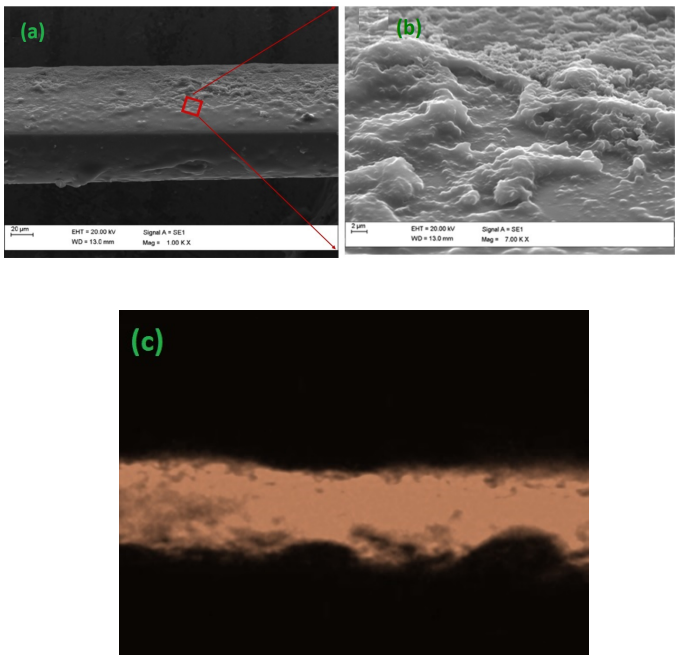

Fig. 3. (a) SEM image of few layered $MoWS_2$ coated on SPF (b) View of magnified region which is noted by the red line (c) confocal image of anti-CTnI monoconal antibody functionalized on $MoWS_2$ coated sensing region

(PBS) (pH 7.4). The SPR spectrum is obtained for $MoWS_2$ nano coated SPF with resonance wavelength of 592±0.02 which is shown in Fig.5. As a first step of incubation process, $MoWS_2$ nano coated SPF is cleaned with PBS and treated with cysteamine solution (10 mM) in PBS for 1 hours at 4 ° C for cysteamine immobilization on polished region based on self-assembly of antibodies. In order to activate the functionalization of antibodies on side polished region of fiber, 10 ng/ml solution of anti-CTnI in PBS is injected inside the microfluidic chamber at a flow rate of 0.5 nL/min for 20 minutes. After that, the sensing region was rinsed with PBS to eliminate the unbound antibodies. 0.05% (w/v) BSA in PBS is used for surface passivation. BSA is injected with a flow rate of 10 μL/min for 10 mins to block unreacted remaining cysteamine to avoid the unspecific adsorption on the sensing region. The incubation period for cTnI antibodies is noted as approximately 30 minutes. Fig.3(c) shows the uniform fluorescence signalling of anti-CTnI functionalized over $MoWS_2$ nano layers and sensing region which inferred through confocal laser microscopy. This result shows the successful functionalization of anti-CTnI antibodies over $MoWS_2$/SPF. Thus, the presence of $MoWS_2$ nanosheets reduces the necessity for cross-linkers and decreases the required incubation time for biofunctionalization process. Moreover, the transmission spectrum is measured after incubation of anti-CTnI for 15 minutes of PBS addition in the microfluidics chamber. Further,

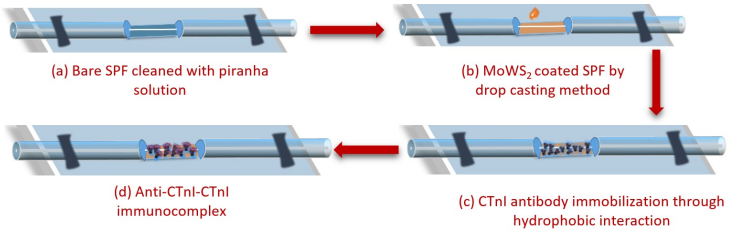

Fig. 4. Schematic view of the development process of $MoWS_2$ nanolayer coating and bioanayte functionalization on SPF biosensor.

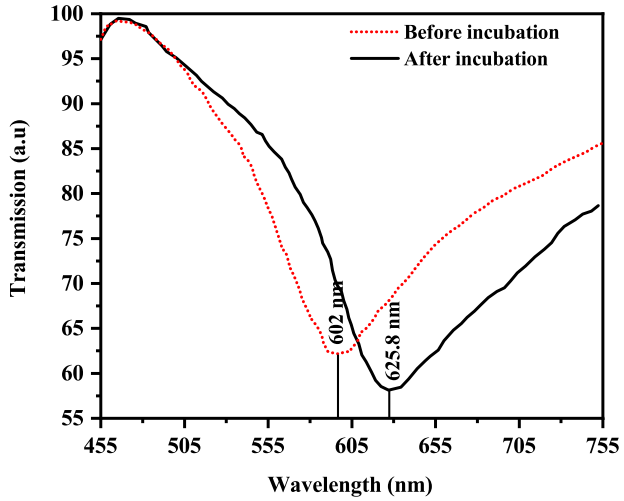

Fig. 5. Spectral characteristics of the $MoWS_2$ nano coated SPF before and after bioanayte functionalization.

the resonance wavelength is noted as 625.8±0.02 nm. The same is depicted in Fig.5

Subsequently, human serum (Sigma-Aldrich, Bangalore, India) is

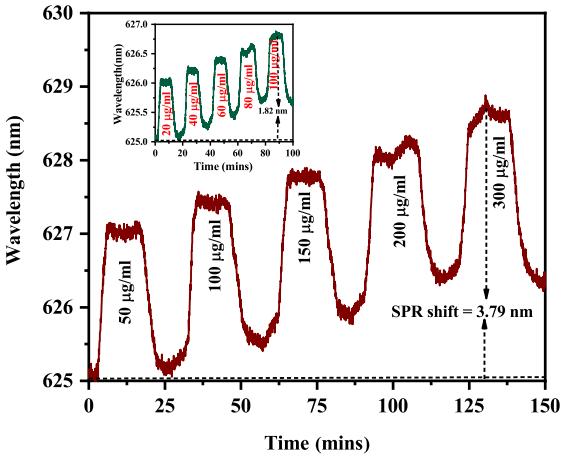

Fig. 6. Sensorgram of $MoWS_2$ nano coated SPR biosensor for various concentration human serum in PBS without any specific analyte.

diluted with PBS in the range of 1:5 for all the experiment work. The dilution range has been fixed based on clinical protocol concern to the human samples to alleviate the matrix effect [30]. This diluted human serum without the spike of any specific analyte is injected by use of BP7 tubing pumps (Bartels & co, Germany) with a concentration ranges from 100 pg/ml to 500 pg/ml. The wavelength shift occur in PBS alone is considered as baseline (625.58 nm). The result of wavelength shift after injection of human serum at the concentration ranges from 50 to 300 μg/mL without any specific analyte is recorded which shown in Fig.6. It is clear from the figure that the mimimum and maximum SPR wavelength shift is 1.79±0.01 nm and 3.79 ±0.03 nm which is minimal. Further, the same test has been repeated for concentration ranges from 20 to 100 μg/mL which is depicted in insets of Fig.6. The same linear response is observed between Fig.6 and its insets and maximum wavelength shift is inferred as 1.82 nm.

C. Expertimental

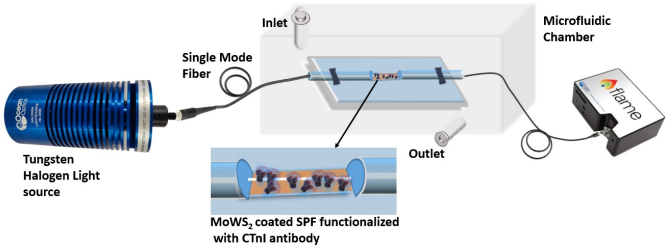

Fig. 7. Experimental setup for biosensing of cTnI antibody

Fig.7 demonstrate the experimental setup of fabricated $MoWS_2$ nano coated SPR biosensor to detect the CTnI antibody. The sensor configuration (Anti-CTnI antigen/ $MoWS_2$/SPF) was positioned within a PDMS microfluidic chamber which featured with a single inlet and outlet. This microfluidic chamber has the external and flow cell temperature as stable as around 25±1 °C and 30±0.05°C, respectively. A light source which have broad wavelength spanning ranges from 360 to 2400 nm and an output power of approximately 8.8 mW (Ocean Optics, HL-2000), was utilized to inject white light into a one face of the SPF biosensor. The transmission characteristics were recorded by a spectrometer, which has a wavelength range from 350 to 1000 nm and a resolution of about 10 nm (Ocean Insight, FLAME-T-VIS-NIR), connected to the opposite face of the SPF. Additionally, the spectrometer was interfaced with a computer to record the spectral characteristics corresponding to various CTnI antigen concentrations. The assay injection proceeds with various concentrations of CTnI solutions, ranging from 100 pg/mL to 500 pg/mL for 15 minutes each at a flow rate of 10 μL/min inside the microfluidic chamber. Between each injection, a washing step using PBS is performed for 5 minutes at a flow rate of 30 μL/min. This step helps to ensure accurate measurement of wavelength shift due to receptor and analyte binding surface interactions as well as eliminate the volumetric effects related to the refractive index of the solution.

IV. Results and Discussion

Fig.8(a) shows the wavelength shift of proposed $MoWS_2$ SPR based biosensor for the CTnI protein spiked human serum with a concentrations ranging from 100 pg/mL to 500 pg/mL. It can be seen from Fig.8(a) that the minimum and maximum resonant wavelength shift is observed as 19.2 ± 0.01 nm at 100 pg/mL and 61± 0.03 nm at 500 pg/mL, respectively. The higher wavelength shift of 61 nm indicates the changes in RI which mainly relies on CTnI receptor and analyte interaction as well as the interaction of evanescent field between surrounding medium and side polished region. The same process has repeated with identical and independent sensor after complete washing with PBS for the concentration from 100 pg/ml to 300 pg/ml for 100 minutes which is shown in insets of Fig.8(a). It is observed that the proposed $MoWS_2$ SPR biosensor possess the same linear characteristics as same as the response for concentration from 100 to 300 pg/mL(minimum and maximum wavelength shift noted as 9.25 nm and 31.15 nm,respectively).Thus, the results show that the proposed sensor exhibit a good response even for the repeatable and reproducible process.

Fig.8(b) shows the error bar graphs illustrating the linear increase in resonance wavelength with increase of CTnI concentration in diluted human serum. The error bars represent the measurements obtained from three identical and independent sensors (n = 3) to evaluate the repeatability and reproducibility of the proposed biosensor. The $MoWS_2$ nano coated SPR device demonstrates a response to

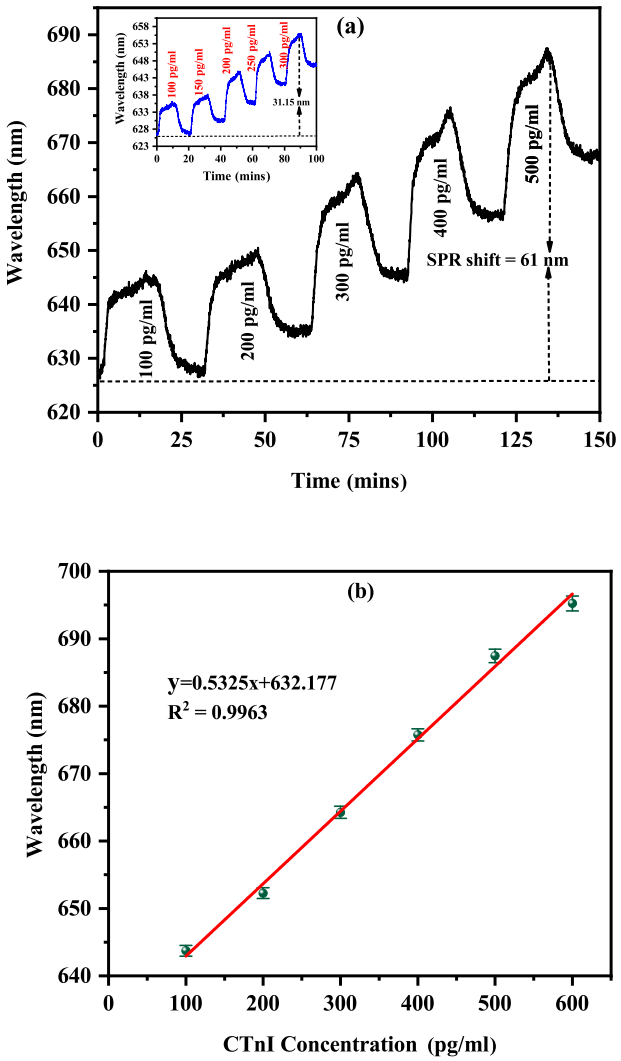

Fig. 8. (a)Sensorgram of $MoWS_2$-nano-coated SPR biosensor for various concentration of CTnT antigen.(b) Spectral behaviour of proposed $MoWS_2$-nano-coated SPR biosensor for various concentration of CTnT antigen. (c) SPR Spectral shift for various concentration of CTnT antigen.

CTnI in PBS within a concentration ranges from 100 to 600 pg/mL. The resonance wavelength red shift occurs owing to the interaction between CTnI and Anti-CTnI antibodies, forming immune complexes that changes the refractive indices of surrounding nano-material and modify the characteristics of the evanescent wave interaction. The concentration of CTnI is directly proportional to the changes in the refractive indices of surrounding medium, and this changes is reflected in the resonance wavelength shift. Notably, it is clear from the linear fit curve of the proposed SPR biosensor exhibits a LOD as 17.5 pg/mL and R^2 value of 0.9963. The concentration of CTnI is lower than 0.01 ng/mL level indicate the chronicle heart diseases and failure [9].Thus, the proposed $MoWS_2$ nano coated SPF biosensor demonstrates lower concentration LOD as 17 pg/mL compared to the cut-off value (0.01 nm/mL). The enhanced lower concentration LOD can be achieved by the large surface-to-volume ratio of grafted few layer $MoWS_2$ on sensing region, which increases the density of functionalized CTnI antibodies binding. Thus, the proposed single

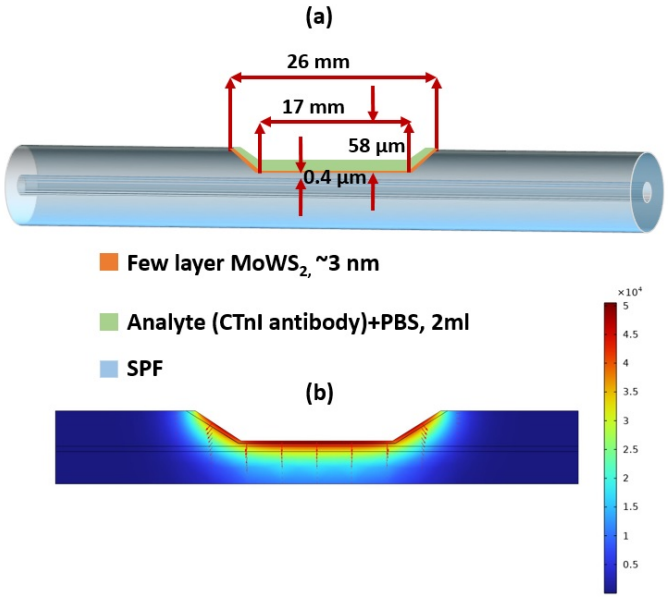

Fig. 9. (a) Schematic view of $MoWS_2$ nanolayer coating and bioassay functionalized SPF biosensor and (b) Simulated Surface interaction field profile of $MoWS_2$ nanolayer, CTnI antibody and side polished region.

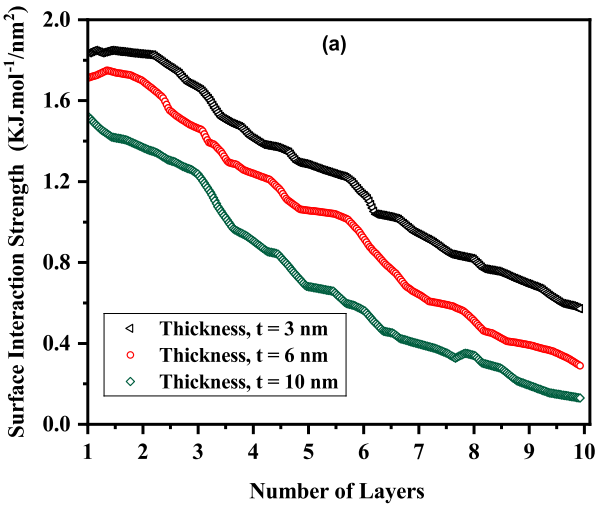

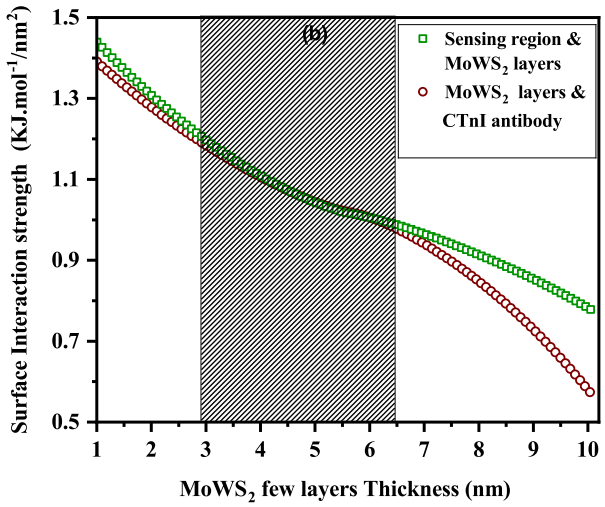

Fig. 10. (a) Total surface interaction strength among sensing, $MoWS_2$ nano coated and CTnI antibodies functionalized region with respect to number of $MoWS_2$ layers for various thickness of same. (b) surface interaction strength between sensing and $MoWS_2$ nano coated region as well as $MoWS_2$ nano coated and CTnI antibodies functionalized region for various thickness of $MoWS_2$ layers.

$MoWS_2$ nano coated SPF biosensor is a promising device to detect the CTnI in order to diagnosis the CVD disorders.

The sensing behaviour of the proposed nano coated SPF biosensor not only rely on the evanescent wave interaction but also hydrophobic nature between few layer $MoWS_2$ and CTnI andibodies. In order to evaluate the hydrophobic interaction, we have use the finite element method (FEM) to calculate the surface interaction strength between $MoWS_2$ and CTnI andibodies. Fig.9(a) illustrates the geometry of the SPF used in this experiment which features has been afore-mentioned in section.III(A). Further, $MoWS_2$ solution was coated on side polished region with various concentration of overlaying of CTnI andibodies. Previously, we have inferred the evanescent field interaction through the experimental results. Nevertheless, the specific quantitative analysis for the determination of hydrophobic interaction to nanomaterials still not evolved [31]. Moreover, the numerical investigation has been analyzed the total surface field interaction for the thickness and numbers of layers of $MoWS_2$. The surface interaction field is depicted in Fig.9(b). Fig.10(a) shows the surface interaction strength for total thickness of $MoWS_2$ nano coating which varied as 3, 6, 10 nm as a function of number of layers mono to few. From Fig.10(a), it is observed that the surface interaction strength has been reduced when the number of $MoWS_2$ layers and total thickness get increased. This is because increase in free energy of the $MoWS_2$ coated surface and reduced surface smoothness when thickness and number of layers gets increased.

The chemical free direct binding affinity of few layer $MoWS_2$ and CTnI antibodies are verified by surface interaction strength. Fig.10(b) indicates the surface interaction strength between sensing and $MoWS_2$ nano coated region as well as $MoWS_2$ nanocoated and CTnI antibodies functionalized region with respect to the $MoWS_2$ total layers thickness. One can observe from Fig.10(b) that the merging of trends occur that the $MoWS_2$ layers thickness from 2.89 to 6.46 nm. This result indicates the hydrophobic interaction of $MoWS_2$ nano layers between sensing and CTnI andibodies. These results has been achieved due to minimized free energy of the $MoWS_2$ surface interface with sensing region and CTnI andibodies. Thus, the results of numerical investigation emphasize the strong hydrophobic interaction $MoWS_2$ few layered surface from 2.89 to 6.46 nm. As has been mentioned earlier that the experimentally confirmed total thickness of the $MoWS_2$ layers is about $\approx$ 3 nm and single layer thickness in 0.615 nm. Hence, number of layers associated with coated $MoWS_2$ is ≈ 5. Wherefore, we have calculated total surface interaction strength as 1.29 KJ mol^{-1}/nm^2 for the 3 nm thickness which corresponds to the number of layers as 5. Therefore, The proposed few layer $MoWS_2$ coated SPF exhibits the chemical free and direct affinity of CTnI antibodies functionalization over the sensing region due to hetrostructure hydrophobic interaction.

Fig.11(a) depicts the selectivity analysis of proposed biosensor which involving various analyte such as CTnI, Glucose and Estrogen in human serum which diluted with PBS in the range of 1:5. The 100 pg/ml and 500 pg/ml concentration of analytes is measured and the difference between the absorbance wavelength of SPR spectra peak (λ_a) at a concentration of 500 pg/ml to 100 pg/ml is calculated.

One can observe from Fig.11(a) that the difference of λ_a between 500 pg/ml to 100 pg/ml is higher for CTnI (61 nm) than Glucose (1.05 nm) and Estrogen (2.22 nm). On the same hand, the inset of Fig.11(a) represents the difference of λ_a between 300 pg/ml to 100 pg/ml is higher for CTnI (30.31 nm) than Glucose (0.52 nm) and Estrogen (1.02 nm). Consequently, we confirm from the result that the proposed $MoWS_2$ nano-coated SPR biosensor possess high selectivity compared to other analytes. This findings supports that the proposed SPF biosensor holds potential as a reliable device for CTnI antibody sensing applications.

The specificity and stability test of proposed SPF biosensor has been conducted at a wavelength of 658 nm (laser diode, RLS/658NM-1000MW) with a wavelength shift measurement of 61 nm which has shown in Fig.11(a), demonstrates the superior response of $MoWS_2$-based biosensors to CTnI antigen compared to other analytes.

Subsequently, it was imperative to assess its stability to ascertain the sensing reliability in the case of prototype development. Consequently, the $MoWS_2$-based biosensor was subjected to continuous testing with CTnI, Glucose and Estrogen analytes for 25 days at a concentration of 500 pg/ml, with results presented in Fig.11 (b). Over this duration, the proposed biosensor wavelength shift experience the marginal decreases of 0.39%, 0.44%, and 0.52% for CTnI, Estrogen and Glucose analytes, respectively, from their initial values. These results shows the robust durability of the proposed bio sensor, thereby laying the groundwork for the advancement of a dependable optical based biosensing device for CVD disorders.

To assess the cross-sensitivity of the proposed SPF biosensor, two groups of analyte concentrations were employed. The initial group included concentrations of 100 pg/mL for CTnI, 200 pg/mL for Glucose, and 400 pg/mL for Estrogen, while the second group consisted of concentrations at 100 pg/mL, 300 pg/mL, and 500 pg/mL. During the experiment, the sensitivity of CTnI consistently remained high for both sets, indicating the reproducibility and consistency of the proposed SPF biosensor. Ultimately, experimantal and simulation result findings indicate the potential efficiency of the proposed $MoWS_2$ coated SPF biosensor for CTnI antibody detection. Thus, the proposed $MoWS_2$-nano-coated SPR biosensor is an excellent candidate for POC accurate diagnosis of cardio diseases.

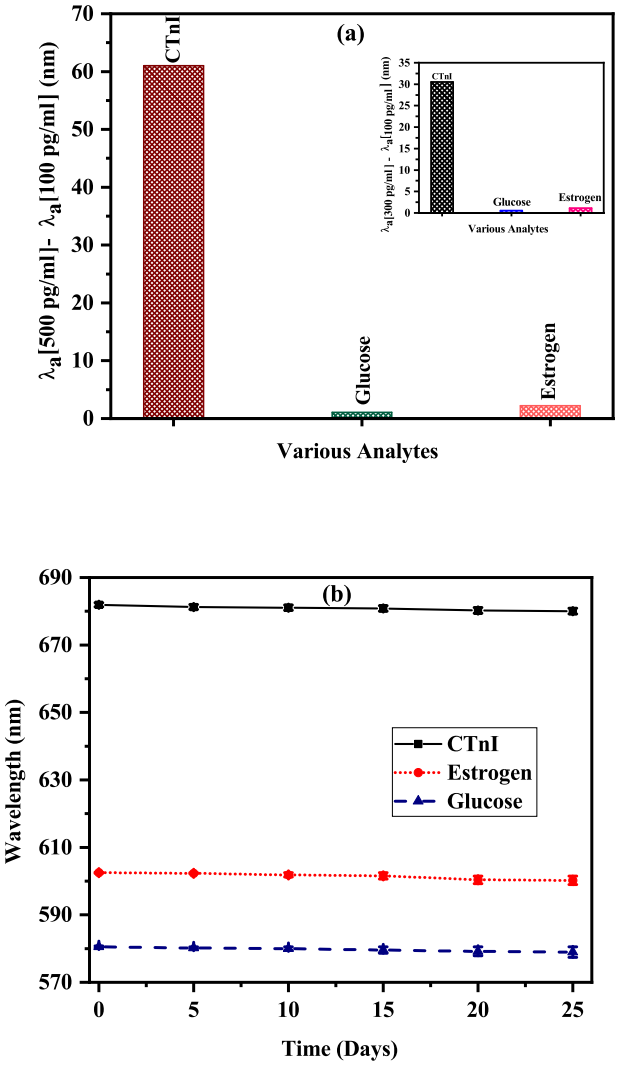

Fig. 11. Test for to analyze the (a) selectivity and (b) stability of proposed $MoWS_2$-nano-coated SPR biosensor for various analytes presents in human serum.

V. Conclusion

In this work, we have demonstrated a high sensitive $MoWS_2$ nanolayers coated side SPF biosensor for early and accurate diagonsis of CVD. Intially, a heterogeneous TMD nanomaterial ($MoWS_2$) is synthesized using the hydrothermal exfoliation method. The side polished region is functionalized with $MoWS_2$ nanolayers and antibodies was characterized by different techniques such as HR-TEM,FESEM, EDX,XRD, UV-Vis spectroscopy and confocal microscopy,respectively. Further, cTnI have chosen as a biomarker for early and fast diagnosis of CVD. The proposed SPF biosensor explore a SPR based detection due to the interaction between $MoWS_2$ nano material coated side polished region and evanescent field. Besides, the proposed SPF biosensor offers the high sensitivity of 82 % with a LOD as 17.5 pg/mL for detection of cTnI antibody. The peak SPR shift have been calculated as 61 nm for very low analyte concentrations of 500 pg/mL due to the strong interaction of evanescent field with cTnI in the side polished region. Furthermore, hydrophobic interactions of $MoWS_2$ and cTnI antibody leads to chemical free direct biofunctionalization of antibody in the sensing region. Moreover, hydrophobic interactions have analyzed through numerical simulation that results shows the surface interaction strength as 1.29 KJ mol^{-1}/nm^2. Additionally, the proposed biosensor demonstrates a high level of sensitivity (peak wavelength shift = 61 nm) to cTnI among the various analytes tested, along with good stability for all three analytes. Thus, The proposed simple biofunctionalization method pave the way to development of optical fiber based SPR biosensor which offering the accessible in "point-of-care" device development and ultra-low concentration analytes based quantitative analysis of CVD.

References

[1] S. Kaptoge, L. Pennells, D. De Bacquer, M. T. Cooney, M. Kavousi, G. Stevens, L. M. Riley, S. Savin, T. Khan, S. Altay, P. Amouyel, G. Assmann, S. Bell, Y. Ben-Shlomo, L. Berkman, J. W. Beulens, C. Björkelund, M. Blaha, D. G. Blazer, T. Bolton, R. Bonita Beaglehole, H. Brenner, E. J. Brunner, E. Casiglia, P. Chamnan, Y.-H. Choi, R. Chowdry, S. Coady, C. J. Crespo, M. Cushman, G. R. Dagenais, R. B. D'Agostino Sr, M. Daimon, K. W. Davidson, G. Engström, I. Ford, J. Gallacher, R. T. Gansevoort, T. A. Gaziano, S. Giampaoli, G. Grandits, S. Grimsgaard, D. E. Grobbee, V. Gudnason, Q. Guo, H. Tolonen, S. Humphries, H. Iso, J. W. Jukema, J. Kauhanen, A. P. Kengne, D. Khalili, W. Koenig, D. Kromhout, H. Krumholz, T. Lam,

G. Laughlin, A. Marín Ibañez, T. W. Meade, K. G. M. Moons, P. J. Nietert, T. Ninomiya, B. G. Nordestgaard, C. O'Donnell, L. Palmieri, A. Patel, P. Perel, J. F. Price, R. Providencia, P. M. Ridker, B. Rodriguez, A. Rosengren, R. Roussel, M. Sakurai, V. Salomaa, S. Sato, B. Schöttker, N. Shara, J. E. Shaw, H.-C. Shin, L. A. Simons, E. Sofianopoulou, J. Sundström, H. Völzke, R. B. Wallace, N. J. Wareham, P. Willeit, D. Wood, A. Wood, D. Zhao, M. Woodward, G. Danaei, G. Roth, S. Mendis, O. Onuma, C. Varghese, M. Ezzati, I. Graham, R. Jackson, J. Danesh, and E. Di Angelantonio, "World health organization cardiovascular disease risk charts: revised models to estimate risk in 21 global regions," *The Lancet Global Health*, vol. 7, no. 10, pp. e1332–e1345, 2019.

[2] H. C. Ates, P. Q. Nguyen, L. Gonzalez-Macia, E. Morales-Narváez, F. Güder, J. J. Collins, and C. Dincer, "End-to-end design of wearable sensors," *Nat Rev Mater*, 2022.

[3] K. Nejati-Koshki, F. Fathi, A. Arabzadeh, and A. Mohammadzadeh, "Biomarkers and optical based biosensors in cardiac disease detection: early and accurate diagnosis," *Anal. Methods*, vol. 15, pp. 5441–5458, 2023.

[4] M. Benford, M. Wang, J. Kameoka, T. Good, and G. Cote, "Functionalized nanoparticles for measurement of biomarkers using a SERS nanochannel platform," in *Plasmonics in Biology and Medicine VII*, T. Vo-Dinh and J. R. Lakowicz, Eds., vol. 7577, International Society for Optics and Photonics. SPIE, 2010, p. 757705.

[5] N. K. Boris, N. B. Daniil, A. B. Nadezhda, Dzantiev, B. Boris, and G. K. Nikolai, "Sers-based lateral flow immunoassay of troponin i by using gap-enhanced raman tags," *Nano Research*, vol. 12, pp. 413–420, 2019.

[6] S. Mabbott, S. C. Fernandes, M. Schechinger, G. L. Cote, K. Faulds, C. R. Mace, and D. Graham, "Detection of cardiovascular disease associated mir-29a using paper-based microfluidics and surface enhanced raman scattering," *Analyst*, vol. 145, pp. 983–991, 2020.

[7] S. Kumar, R. Singh, G. Zhu, Q. Yang, X. Zhang, S. Cheng, B. Zhang, B. K. Kaushik, and F.-Z. Liu, "Development of uric acid biosensor using gold nanoparticles and graphene oxide functionalized micro-ball fiber sensor probe," *IEEE Transactions on NanoBioscience*, vol. 19, no. 2, pp. 173–182, 2020.

[8] A. Bekmurzayeva, Z. Ashikbayeva, Z. Myrkhiyeva, A. Nugmanova, M. Shaimerdenova, T. Ayupova, and D. Tosi, "Label-free fiber-optic spherical tip biosensor to enable picomolar-level detection of cd44 protein," *Sci Rep*, vol. 11, p. 19583, 2021.

[9] T. Liu, L.-L. Liang, P. Xiao, L.-P. Sun, Y.-Y. Huang, Y. Ran, L. Jin, and B.-O. Guan, "A label-free cardiac biomarker immunosensor based on phase-shifted microfiber bragg grating," *Biosensors and Bioelectronics*, vol. 100, pp. 155–160, 2018.

[10] F. Chiavaioli, P. Zubiate, I. Del Villar, C. R. Zamarreño, A. Giannetti, S. Tombelli, C. Trono, F. J. Arregui, I. R. Matias, and F. Baldini, "Femtomolar detection by nanocoated fiber label-free biosensors," *ACS Sensors*, vol. 3, no. 5, pp. 936–943, 2018.

[11] W. Zhang, X. Lang, X. Liu, G. Li, R. Singh, B. Zhang, and S. Kumar, "Advances in tapered optical fiber sensor structures: From conventional to novel and emerging," *Biosensors*, vol. 13, no. 6, 2023.

[12] A. ADS, D. FDS, A. RCSB, and M. Werneck, "Surface plasmon resonance and bending loss-based u-shaped plastic optical fiber biosensors," *Sensors (Basel)*, vol. 18, no. 2, p. 648, 2018.

[13] J. Dong, Y. Zhang, Y. Wang, F. Yang, S. Hu, Y. Chen, W. Zhu, W. Qiu, H. Guan, H. Lu, J. Yu, Y. Zhong, J. Zhang, Y. Luo, and Z. Chen, "Side-polished few-mode fiber based surface plasmon resonance biosensor," *Opt. Express*, vol. 27, no. 8, pp. 11 348–11 360, Apr 2019.

[14] S. Kaushik, A. Tiwari, Umesh K.and Deep, and R. K. Sinha, "Two-dimensional transition metal dichalcogenides assisted biofunctionalized optical fiber spr biosensor for efficient and rapid detection of bovine serum albumin," *Sci. Rep.*, vol. 9, pp. 1–11, 2019.

[15] N. Liu, S. Wang, Q. Cheng, B. Pang, and J. Lv, "Two-dimensional transition metal dichalcogenides-based high sensitivity lossy mode refractive index sensor," *IEEE Sensors Journal*, vol. 21, no. 5, pp. 6043–6049, 2021.

[16] J. Mohanraj, M. Valliammai, S. Sridevi, T. Kanimozhi, N. Vinodhkumar, and S. Sivabalan, "All fiber-optic multigas (NH_3, NO_2, and CO) sensor based on $MoWS_2$ coated fiber," *IEEE Sensors Journal*, vol. 22, no. 13, pp. 12 869–12 876, 2022.

[17] Y. Hu, Y. Huang, C. Tan, X. Zhang, Q. Lu, M. Sindoro, X. Huang, W. Huang, L. Wang, and H. Zhang, "Two-dimensional transition metal dichalcogenide nanomaterials for biosensing applications," *Mater. Chem. Front.*, vol. 1, pp. 24–36, 2017.

[18] L. J. Fang, J. H. Chen, J. M. Wang, W. W. Lin, X. G. Lin, Q. J. Lin, and Y. He, "Hydrophobic two-dimensional mos2 nanosheets embedded in a polyether copolymer block amide (peba) membrane for recovering pyridine from a dilute solution," *ACS Omega*, vol. 6, no. 4, pp. 2675–2685, 2021.

[19] P. K. Chow, E. Singh, B. C. Viana, J. Gao, J. Luo, J. Li, Z. Lin, A. L. Elías, Y. Shi, Z. Wang, M. Terrones, and N. Koratkar, "Wetting of mono and few-layered ws2 and mos2 films supported on si/sio2 substrates," *ACS Nano*, vol. 9, no. 3, pp. 3023–3031, 2015.

[20] H. Ma, A. Cassedy, and R. O'Kennedy, "The role of antibody-based troponin detection in cardiovascular disease: A critical assessment," *Journal of Immunological Methods*, vol. 497, p. 113108, 2021.

[21] M. Valliammai, J. Mohanraj, B. Esakki, L.-J. Yang, C.-C. Wang, and T. Sridarshini, "Nanomaterial coated side polished fiber for early diagnosis of cardiovascular disease by label-free sensing of troponin biomarker," in *2023 IEEE Workshop on Recent Advances in Photonics (WRAP)*, 2023, pp. 1–3.

[22] T. C, G. D, L. C, G. AK, E. S, S. N, S. M, B. T, H. C, and R. A., "Cardiac troponin i: A valuable biomarker indicating the cardiac involvement in fabry disease." *PLoS One*, vol. 15, pp. e0 157 640–652, 2016.

[23] A. S, G. E, J. T, and K. H., "Troponin elevation in coronary vs. non-coronary disease." *Eur Heart J.*, vol. 32, pp. 404–411, 2011.

[24] M. Abdolrahim, M. Rabiee, S. N. Alhosseini, M. Tahriri, S. Yazdanpanah, and L. Tayebi, "Development of optical biosensor technologies for cardiac troponin recognition," *Analytical Biochemistry*, vol. 485, pp. 1–10, 2015.

[25] H. Li, K. Yu, Z. Tang, and Z. Zhu, "Experimental and first-principles investigation of mows2 with high hydrogen evolution performance," *ACS Applied Materials & Interfaces*, vol. 8, no. 43, pp. 29 442–29 451, Oct 2016.

[26] J. H. Appel, D. O. Li, J. D. Podlevsky, A. Debnath, A. A. Green, Q. H. Wang, and J. Chae, "Low cytotoxicity and genotoxicity of two-dimensional mos2 and ws2," *ACS Biomaterials Science & Engineering*, vol. 2, no. 3, pp. 361–367, 2016.

[27] F. Li, J. Li, Z. Cao, X. Lin, X. Li, Y. Fang, X. An, Y. Fu, J. Jin, and R. Li, "Mos2 quantum dot decorated rgo: a designed electrocatalyst with high active site density for the hydrogen evolution reaction," *J. Mater. Chem. A*, vol. 3, pp. 21 772–21 778, 2015.

[28] Z. Luo, Y. Huang, M. Zhong, Y. Li, J. Wu, B. Xu, H. Xu, Z. Cai, J. Peng, and J. Weng, "1-, 1.5-, and 2-μm fiber lasers q-switched by a broadband few-layer mos2 saturable absorber," *J. Lightwave Technol.*, vol. 32, no. 24, pp. 4077–4084, Dec 2014.

[29] C. M. Zhang, R. Howe, I. Woodward, J. E. Kelleher, F. Torrisi, G. Hu, V. S. Popov, J. R. Taylor, and T. Hasan, "Solution processed mos2-pva composite for sub-bandgap mode-locking of a wideband tunable ultrafast er:fiber laser," *Nano Research*, vol. 8, no. 5, pp. 1522–1534, 2015.

[30] B. Zhang, R. Kumar, and H. Dai, "A plasmonic chip for biomarker discovery and diagnosis of type 1 diabetes," *Nat Med*, vol. 20, p. 948–953, Jul 2014.

[31] A. Valsesia, C. Desmet, I. Ojea-Jiménez, A. Oddo, R. Capomaccio, F. Rossi, and P. Colpo, "Direct quantification of nanoparticle surface hydrophobicity," *Communications Chemistry*, vol. 1, no. 1, pp. 1–11, Sep 2018.